Hemodynamic rounds: Transcatheter creation of ventricular septal defect in pulmonary arterial hypertension with suprasystemic pressures

Kothandam Sivakumar
Department of Pediatric Cardiology, Institute of Cardio Vascular Diseases, Madras Medical Mission, Chennai, Tamil Nadu, India

ABSTRACT

This hemodynamic round section deals with severe pulmonary arterial hypertension with suprasystemic pulmonary artery pressures in a patient who underwent delayed surgical correction of the double-outlet right ventricle with a large subaortic ventricular septal defect (VSD). Recreation of a moderate-sized VSD by electrocautery-aided fenestration of the surgical patch resulted in effective right ventricular decompression. The changes in the hemodynamics are illustrated in the pressure traces and Doppler echocardiographic images. The changes in cardiac events on the right and left heart due to the right bundle branch block are also illustrated in the manuscript.

Keywords: Congenital heart disease, double-outlet right ventricle, electrosurgery, interventional treatment of pulmonary hypertension, pulmonary vascular resistance, right ventricular decompression

INTRODUCTION

Congenital heart diseases (CHDs) with shunts lead to increased pulmonary blood flow that predisposes to pulmonary arterial hypertension (PAH).[1,2] While early surgical or interventional correction normalizes the pulmonary pressures in most infants, late interventions in older patients lead to progressive nonreversible vascular changes and fixed pulmonary vascular resistance.[3,4] Marked elevation of pulmonary artery (PA) pressures leads to dilatation and dysfunction of the right ventricle (RV), causing congestive heart failure, syncope, and sudden cardiac death. Interventional management decompresses the right atrium (RA) through balloon atrial septostomy or the PA through a reversed Potts shunt.[5] This hemodynamic round section deals with the hemodynamics in an adult with progressive PAH after delayed closure of a ventricular septal defect (VSD) and the changes after RV decompression by a transcatheter fenestration of the surgical VSD patch. The accompanying hemodynamic traces and echocardiographic images illustrate the changes during different phases of the cardiac cycle.

CASE REPORT

A 20-year-old female presented with a 2-year history of dyspnea on effort, two episodes of exercise-induced syncope, and worsening of functional class to NYHA Class III in the past 2 months. As the echocardiogram showed evidence of severe PAH, she was initiated on macitentan and sildenafil for 2 years without any improvement of symptoms. She was earlier operated on for a double-outlet RV, large subaortic VSD, and severe

Access this article online

Quick Response Code:

Website: https://journals.lww.com/aopc

DOI: 10.4103/apc.apc_211_24

How to cite this article: Sivakumar K. Hemodynamic rounds: Transcatheter creation of ventricular septal defect in pulmonary arterial hypertension with suprasystemic pressures. Ann Pediatr Card 2024;17:448-54.

Address for correspondence: Dr. Kothandam Sivakumar, Department of Pediatric Cardiology, Institute of Cardio Vascular Diseases, Madras Medical Mission, 4A Dr J J Nagar, Mogappair, Chennai - 600 037, Tamil Nadu, India.
E-mail: drkumarsiva@hotmail.com

Submitted: 02-Nov-2024 **Revised:** 15-Dec-2024 **Accepted:** 13-Mar-2025 **Published:** 24-Apr-2025

PAH at 5 years of age at another institution without any prior invasive hemodynamic cardiac catheterization. The early postoperative period was uneventful, and she was lost to medical follow-up for the next 13 years. On clinical examination, she had pulse oximeter saturation of 99% in room air, weighed 51 kg, showed elevated jugular venous pulsations up to 5 cm above the clavicle with prominent "v" waves, left parasternal systolic heave and a grade III tricuspid pansystolic murmur. Chest X-ray showed a cardiothoracic ratio of 55%, an enlarged RA, and a prominent main PA segment [Figure 1]. There was a right axis deviation of the QRS axis to 165°, a right bundle branch block (RBBB), and RV hypertrophy on the electrocardiogram (ECG) [Figure 2]. Echocardiogram showed congested inferior caval vein and hepatic veins, persistent left superior caval vein draining to the coronary sinus, right atrial and ventricular dilatation, RV systolic dysfunction, moderate tricuspid regurgitation, predicted RV systolic pressures of 150 mmHg, intact ventricular septum, and dilated pulmonary arteries [Figure 3].

Hemodynamic data

Cardiac catheterization was performed after optimal intravenous diuretics for 3 days to control heart failure and triple pulmonary vasodilator therapy, including selexipag. The right atrial mean pressure was 8 mmHg and showed tall v waves of 14 mmHg [Figure 4]. RV and left ventricular end-diastolic pressures were 15 and 8 mmHg, respectively [Figure 5]. The PA pressure was 165/90 (120) mmHg compared to 95/60 (75) mmHg aortic pressures [Figure 6]. PA saturation of 52.3% compared to aortic saturation of 93.2% indicated high oxygen extraction and a low cardiac output of 1.8 l/m. Oxygen consumption derived from Lafarge charts in this 20-year-old female with a heart rate of 56/min was 106 ml/min/m^2. There was no step-up or step-down in oximetry, indicating a lack of any residual shunts. The indexed pulmonary vascular resistance was 62 WU.m^2, and the pulmonary-to-systemic resistance ratio was 1.6. There was no fall in pulmonary pressures on acute vasodilator testing using inhaled nitric oxide. The left ventricular contrast angiogram in the left anterior oblique view showed intact ventricular septum and lack of residual shunt [Figure 7].

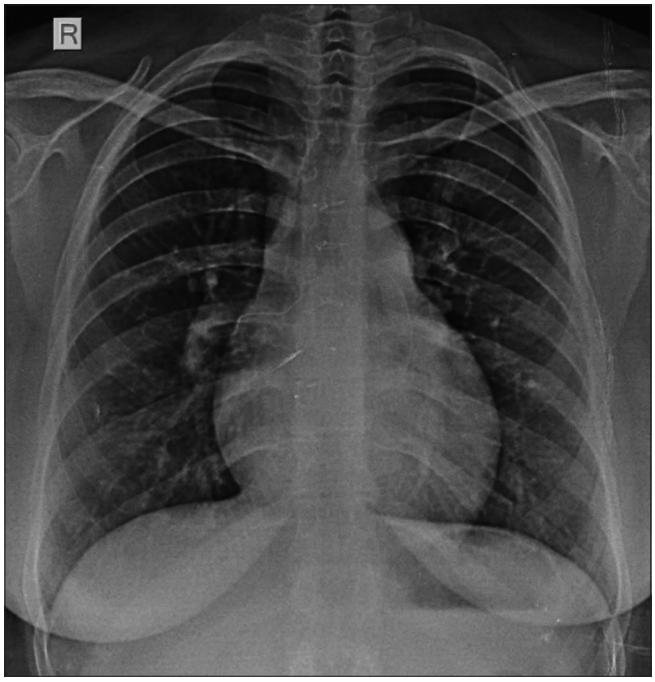

Figure 1: Chest X-ray shows mild cardiomegaly, right atrial and main pulmonary artery segment enlargement

Interventional options

Progressive symptoms of effort-induced dyspnea and syncope despite optimal pulmonary vasodilator therapy warranted add-on interventions. Balloon atrial septostomy might eliminate or reduce episodes of exercise-induced syncope at the cost of systemic desaturation.[6] A controlled atrial septal fenestration could be effectively created using atrial flow-regulator devices.[7] As the right atrial pressures of 8 mmHg in this patient were similar to the left ventricular end-diastolic pressures, atrial septostomy would not be expected to lead to a substantial right-to-left shunt and significant hemodynamic improvement.[8] Marked variations between the two ventricular systolic pressures would indicate a possibility of significant hemodynamic improvement after a posttricuspid decompression. A reversed transcatheter Pott's shunt might favorably reduce the pulmonary and RV pressures.[9] However, this procedure carried high procedural morbidity risks.[10]

Direct right ventricular decompression

Transcatheter creation of VSD is anecdotally described in infants with elevated systemic ventricular pressures but not reported in patients with suprasystemic PAH.[11,12] After discussing our patient details, the heart team decided to proceed with transcatheter perforation of the previous surgical VSD patch and enlarging the orifice with a large balloon. Contrast computed tomographic imaging profiled the previous VSD patch and its relationship to the aortic root on the left side and the tricuspid valve (TV)

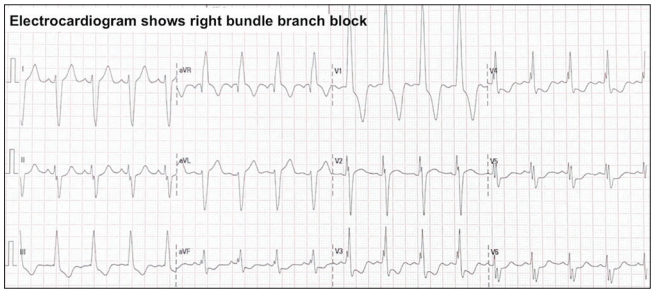

Figure 2: Electrocardiogram shows right axis deviation, right bundle branch block, and right ventricular hypertrophy

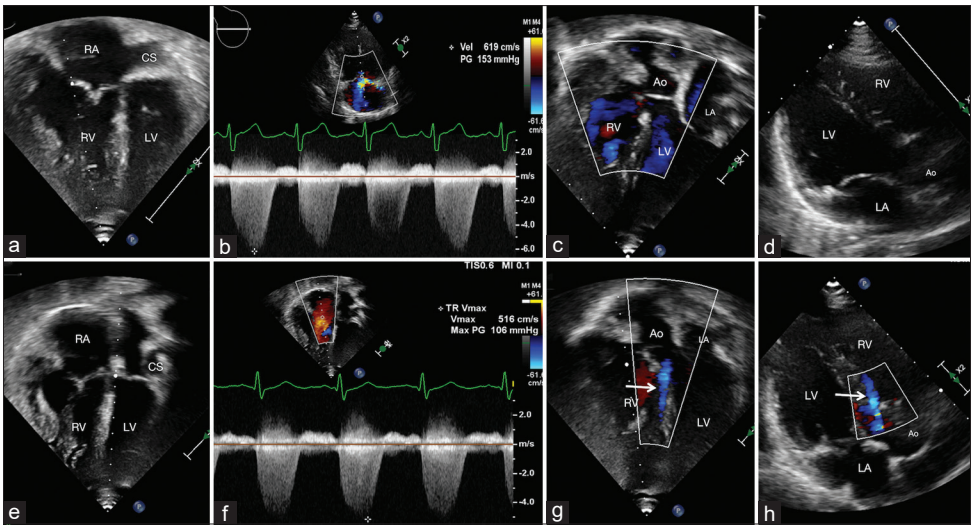

Figure 3: Echocardiogram before the intervention (a-d) shows dilated right ventricle (RV) and right atrium (RA) on apical view (a), RV systolic pressure of 153 mmHg (b) by tricuspid regurgitation Doppler, no residual ventricular septal defect on five-chamber view (c) and unobstructed left ventricular outflow on parasternal long axis view (d). After the intervention (e-h), similar views show a reduction in size of RA and RV (e), RV systolic pressure of 106 mmHg (f), right to left shunt through the fenestration shown in white arrow in the surgical patch on apical five-chamber (g) and parasternal long axis view (h) into the left ventricle. Ao: Aorta, CS: Coronary sinus; LA: Left atrium, RV: Right ventricle, RA: Right atrium

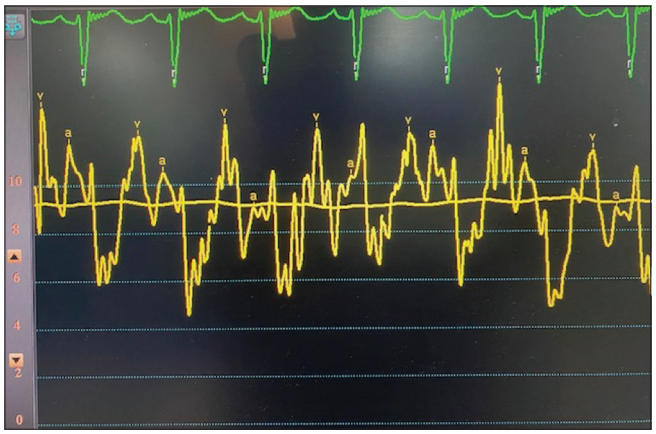

Figure 4: The right atrial pressure trace shows prominent v waves measuring 14 mm of mercury during mid-systole after the R wave of the electrocardiogram, indicating the significance of tricuspid regurgitation and a mean atrial pressure of 8–9 mm of mercury

apparatus on the right side [Figure 8]. It confirmed RV dilatation, bowing of the ventricular septum to the left, and mild aortomitral discontinuity, which is in agreement with the original diagnosis of double outlet RV. Fenestration should be placed away from the aortic valve to avoid a distortion of the aortic annulus and damage to the leaflets. As the atrioventricular conduction tissue was predicted to course along the posterior margin of the VSD patch, the direction of perforation of the patch should be directed anteriorly and apically to maintain a safe distance from the aortic annulus and the conduction tissue. Electrosurgery would be needed to deliver radiofrequency energy through the perforating wire tip to fenestrate the old fibrosed pericardial surgical patch.[13] Injury to the aortic valve leaflets by the radiofrequency energy from the sides of the guidewire should be prevented by a transarterial sheath placed beyond the aortic valve annulus. Placement of stents near the vicinity of the VSD surgical patch to reinforce the perforation might lead to injury to the left ventricular outflow (LVOT) tract as well as the TV apparatus. Hence, it was decided to dilate the perforation using a large balloon instead of placing stents.

Interventional details

After a left ventriculogram delineating the VSD patch on a long axial view, an arterial 6F long flexor sheath (Cook Medical, Bloomington, IN, USA) was placed in the LVOT tract beyond the aortic root to avoid injury to the aortic valve leaflets by the radiofrequency energy. A 5F internal mammary catheter was advanced through the long sheath and torqued to maintain contact with the anterior and apical end of the surgical patch guided on the left anterior oblique and lateral projection of fluoroscopy [Figure 7]. A 0.014" Conquest Pro Guidewire (Asahi Intecc, Tokyo, Japan) was placed over a FineCross MG microcatheter (Terumo Corporation, Tokyo, Japan) within this catheter. Electrical energy on cutting mode was delivered to the tip of the coronary wire from its back end at 40 Watts for 4 s to perforate the surgical VSD patch. After advancing the microcatheter over the wire, a contrast injection confirmed the tip of the catheter was in the RV on echocardiography. The guidewire was exchanged for a Run-through NS 0.014" extra floppy wire (Terumo Corporation, Tokyo, Japan). This wire was snared from the venous end through a catheter in the RA. The perforation in the surgical VSD patch was serially dilated with 2 mm and 4 mm coronary

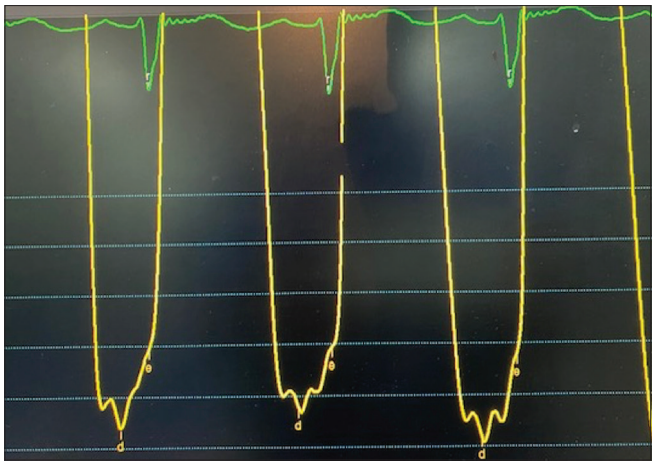

Figure 5: Right ventricular pressure trace shows elevated end-diastolic pressure of 15–20 mm of mercury, demonstrated by the letter (e) corresponding to the R wave of the electrocardiogram

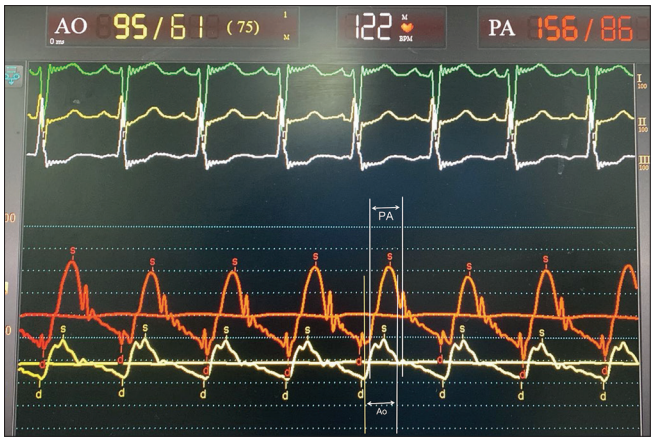

Figure 6: Simultaneous ascending aortic (yellow) and pulmonary artery (PA) (red) pressures show suprasystemic PA pressures. The phase delay between the arterial systolic phases ending with dicrotic notches reflects the delay in pulmonary arterial pulse due to the right bundle branch block and the resultant delay in right ventricular ejection

balloons before advancing a diagnostic catheter across the patch from the left ventricular end. This catheter allowed placement of an Amplatz super-stiff 0.035" wire (Boston Scientific, Natick, MA, USA) from the arterial end. The fenestration was progressively dilated with an 8 mm Mustang balloon (Boston Scientific, Natick, MA, USA) followed by a 14 mm Atlas Gold balloon (Bard Peripheral Vascular, Tempe, AZ, USA) to achieve a final orifice of around 8 mm measured on echocardiography after the final inflation. The procedure was stopped once the right ventricular pressures equaled the femoral artery pressure, indicating sufficient decompression of the RV. The decrease in oxygen saturation to 85% was managed by high-flow supplemental oxygen for the next 24 h. Packed red blood cells were transfused to improve the hemoglobin from 10 g/dl to 14 g/dl to ensure sufficient tissue oxygen delivery. Blood gas analysis confirmed the absence of metabolic acidosis and tolerance to the new-onset hypoxia from the fenestration. No oximetry run was performed as the echocardiogram showed a shunt across the newly created VSD patch fenestration. Fick oximetry might be unreliable in precisely predicting the right-to-left shunt in acutely created shunts. Pharmacotherapy was continued with triple pulmonary vasodilators.

Hemodynamics on echocardiography

The created fenestration measured 8 mm and was located at the apical, anterior end of the surgical patch [Figure 3]. The VSD showed a right-to-left shunt with a mid-systolic gradient of 15 mmHg between the two ventricles. There was a significant reduction of RV systolic pressures to 106 mmHg compared to simultaneous right arm cuff blood pressures of 100/60 mmHg. The dilatation and systolic function of the RV showed improvement compared to the preprocedural images. Doppler interrogation of the right-to-left shunt through the fenestration showed nearly equal ventricular systolic pressures, indicating significant RV decompression [Figure 7]. There was no congestion of the inferior caval or hepatic veins.

Cardiac cycle timings with Doppler echocardiography

The Doppler trace across the VSD fenestration showed a triphasic systolic pattern [Figure 9]. There was an early systolic left-to-right flow, a mid-systolic right-to-left flow at a lower velocity, and a late systolic right-to-left flow at a marginally higher velocity. The postprocedural ECG showed a complete RBBB, which led to the initiation of left ventricular systole earlier than the RV. This caused the initial left-to-right shunt in the first 120 ms after the R-wave on the ECG. As the RV systole started after this first phase, the midsystolic right-to-left flow indicated the low interventricular gradient and near equalization of the ventricular pressures. In late systole due to RBBB, the RV contraction continued for a few milliseconds even after the early diastolic decline of the left ventricular pressures. This marginally caused an augmentation of the right-to-left interventricular gradient in the last three phases. The impact of the RBBB was seen in the hemodynamic traces as well [Figure 10]. In simultaneous RV and aortic pressure traces, there was a late systolic peaking of the RV pressures compared to early systolic peaking of the aortic pressures. A simultaneous display of the left ventricular and PA pressures demonstrated an early peak of the former and a late peak of the latter, demonstrating the influence of the RBBB.

DISCUSSION

PA pressures are markedly elevated in large posttricuspid shunt lesions due to combined pressure and volume overload on the pulmonary vasculature. The resultant vascular changes result from a dynamic multifactorial

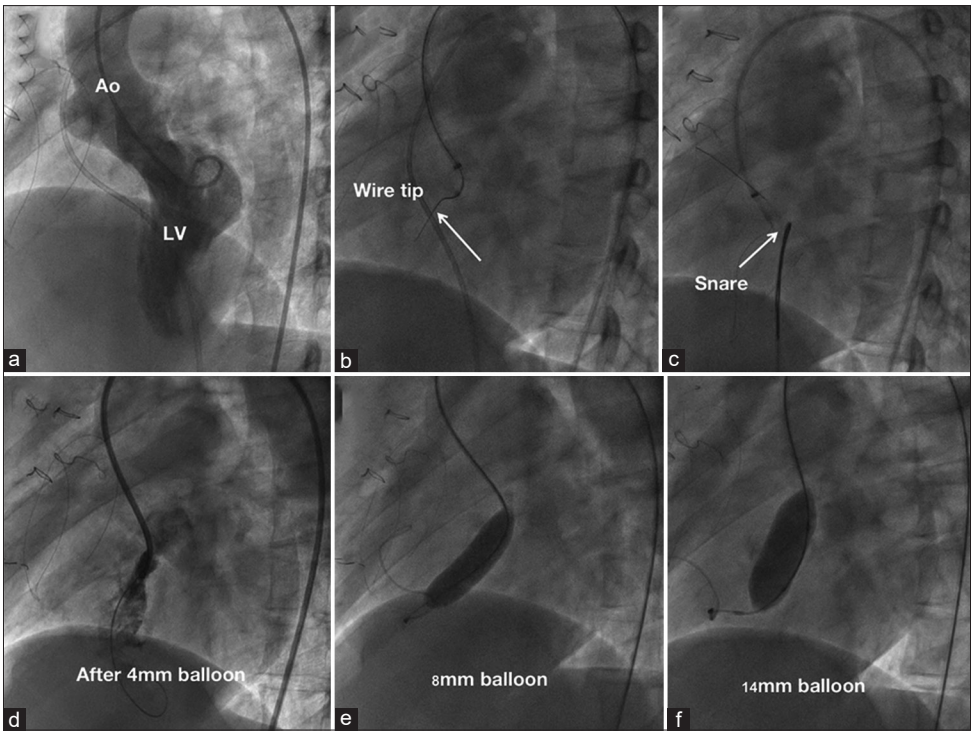

Figure 7: Left ventriculogram in left anterior oblique view (a) shows the absence of residual ventricular septal defect (VSD). A chronic total occlusion coronary wire placed within a microcatheter was advanced from the tip of an internal mammary artery catheter towards the anterior-apical part of the VSD patch aided by electrosurgery (b), and the tip of the coronary wire was snared in the right ventricle (c). After initial dilatation of the created fenestration with coronary balloons (d), the fenestration was further enlarged with 8 mm (e) and 14 mm (f) balloons to create a larger right ventricular decompression. Ao: Aorta, LV: Left ventricle

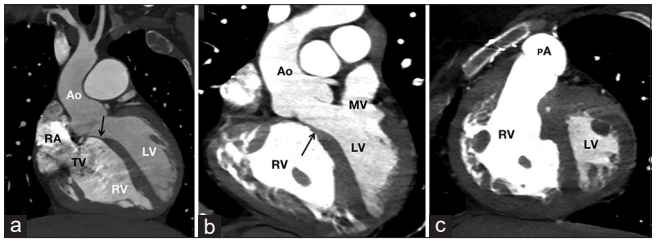

Figure 8: Contrast computed tomographic images show dilated right atrium and right ventricle (RV), surgical patch in the ventricular septal defect shown in arrow in (a and b), its close relation to tricuspid valve and aortic valve. The interventricular septum in panels (b and c) bows into the left ventricle, indicating high RV and pulmonary artery pressures. Ao: Aorta, LA: Left atrium, RV: Right ventricle, RA: Right atrium, PA: Pulmonary artery, MV: MV mitral valve, RA: Right atrium

process with progressive endothelial dysfunction, vasoconstriction, and remodeling.[1] Delayed surgery in the presence of established "fixed" PAH may lead to progressive elevation of pulmonary vascular resistance, accelerate the disease progress, and onset of RV failure.[2] A "point of no return" in the changes of pulmonary vasculature may occur despite correction of the associated defect.[3] Anatomical–pathophysiological classification of CHD associated with PAH lists operated patients with persistent vascular disease as Class D.[4] The prognosis of this group is considered worse than the other forms of CHD-associated PAH.[14] Postoperative PAH is associated with high morbidity, mortality, and increased health service utilization despite recent advances in pharmacotherapy.[15] PAH-CHD remains the second most common cause of associated PAH in clinical practice.[16]

Balloon atrial septostomy and reversed Potts shunt are two interventions available to rescue patients with severe PAH when they present with syncope or RV failure.[5] Atrial septostomy maintains systemic cardiac output at the cost of systemic hypoxia, effectively preventing syncope from a pulmonary hypertensive crisis.[6] Atrial flow regulators are proven to improve outcomes and survival in these patients. When the failing RV functions in the declining limb of the Frank–Starling curve, atrial septostomy reduces the RV filling and shifts it to the left of the curve.[7] Potts shunt directly reduces the PA and RV systolic pressures, thus effectively lowering the RV afterload. Lack of cerebral hypoxia is a significant advantage of Potts shunt compared to atrial septostomy. Still, its main downside is reduced filling of the left ventricle, which may reduce stroke volume.[5] Some patients develop precipitous systemic hypotension that may warrant strong vasopressors to increase systemic vascular resistance after the Potts shunt. Severe pulmonary and tricuspid regurgitation, common accompaniments of severe PAH, may preclude Potts shunt.[5]

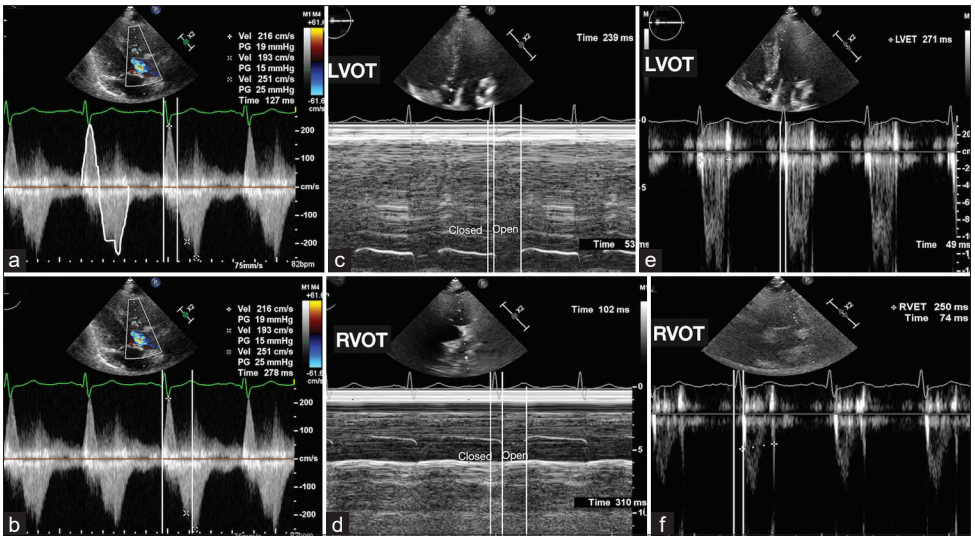

Figure 9: Spectral Doppler trace of flow through the ventricular septal defect fenestration show a triphasic pattern (a) with first left to right component lasting initial 120 ms, second right to left component at low velocity lasting 160 ms (b) and third right to left component at marginally higher velocity toward the end of systole. M-mode interrogation of left ventricular outflow and right ventricular outflow shown in (c and d) demonstrate the opening and closing of the aortic and pulmonary valves, respectively. Due to the right bundle branch block, the pulmonary valve opens 102 ms after the Q wave and closes 310 ms later. On the contrary, the aortic valve opens 53 ms after the Q wave and closes at 239 ms. Spectral Doppler signal across the aortic (e) and pulmonary (f) annulus also shows the delay in onset of right ventricular ejection (74 ms) compared to left ventricular ejection (49 ms) due to right bundle branch block. LVOT: Left ventricular outflow, RVOT: Right ventricular outflow

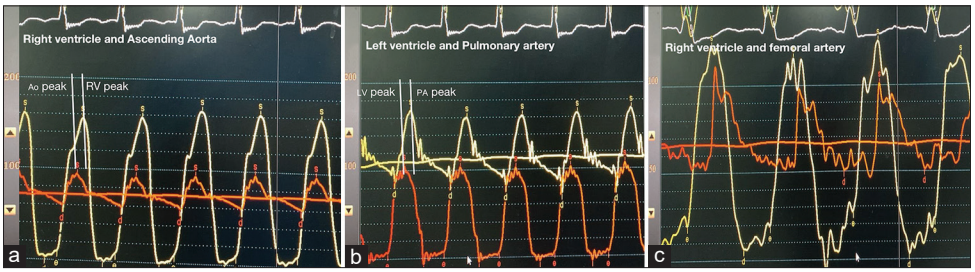

Figure 10: Simultaneous right ventricular and ascending aortic pressure trace (a) shows right ventricular systolic pressure is more than 60 mmHg above the aortic systolic pressure. The vertical bars show the peak right ventricular pressure phase delay due to the right bundle branch block (RBBB). Similar simultaneous left ventricular and pulmonary artery pressure traces (b) show suprasystemic pulmonary pressures and delay in pulmonary artery peak compared to the left ventricular peak shown by vertical bars due to the RBBB. After the creation of fenestration in the ventricular septal defect patch, a fall in the right ventricular systolic pressure trace compared to the femoral artery pressure trace (c) shows effective right ventricular decompression. Femoral artery trace is delayed compared to the right ventricle due to the natural delay in the pulse wave to reach the distant vessels. Ao: Aorta, RV: Right ventricle, PA: Pulmonary artery, LV: Left ventricle

Direct RV decompression in patients with severe PAH has not been described in the literature so far. Transcatheter fenestration of the surgical VSD patch is yet another potential target in the interventional armamentarium of these patients. While previous reports of transcatheter VSD creation using balloon expandable stents in the muscular septum targeted young infants with restrictive VSD in patients with complex cyanotic CHDs, our approach was to fenestrate the surgical VSD patch.[11,12] The anteroapical end of the patch was chosen for perforation as it would maintain a safe distance from the aortic valve leaflets, tricuspid apparatus, and atrioventricular conduction tissues. The hemodynamic changes shown in the pressure traces and Doppler echocardiography help understand the labile changes during this intervention.

Declaration of patient consent

The authors certify that they have obtained all appropriate patient consent forms. In the form, the patient has given her consent for her images and other clinical information to be reported in the journal. The patient understand that name and initials will not be published and due efforts will be made to conceal identity, but anonymity cannot be guaranteed.

Ethics approval statement

Complied with all ethical standards of the institutional protocols.

Author contribution

The author contributed to the concept, data analysis, drafting, revision, and article approval.

Financial support and sponsorship

Nil.

Conflicts of interest

There are no conflicts of interest.

REFERENCES

1. Humbert M, Sitbon O, Simonneau G. Treatment of pulmonary arterial hypertension. N Engl J Med 2004;351:1425-36.
2. Haworth SG. Pulmonary hypertension in the young. Heart 2002;88:658-64.
3. D'Alto M, Mahadevan VS. Pulmonary arterial hypertension associated with congenital heart disease. Eur Respir Rev 2012;21:328-37.
4. Galiè N, Hoeper MM, Humbert M, Torbicki A, Vachiery JL, Barbera JA, *et al.* Guidelines for the diagnosis and treatment of pulmonary hypertension: The task force for the diagnosis and treatment of pulmonary hypertension of the European Society of Cardiology (ESC) and the European Respiratory Society (ERS), endorsed by the International Society of Heart and Lung Transplantation (ISHLT). Eur Heart J 2009;30:2493-537.
5. Stącel T, Latos M, Urlik M, Nęcki M, Antończyk R, Hrapkowicz T, *et al.* Interventional and surgical treatments for pulmonary arterial hypertension. J Clin Med 2021;10:3326.
6. Rajeshkumar R, Pavithran S, Sivakumar K, Vettukattil JJ. Atrial septostomy with a predefined diameter using a novel occlutech atrial flow regulator improves symptoms and cardiac index in patients with severe pulmonary arterial hypertension. Catheter Cardiovasc Interv 2017;90:1145-53.
7. Sivakumar K, Rohitraj GR, Rajendran M, Thivianathan N. Study of the effect of occlutech atrial flow regulator on symptoms, hemodynamics, and echocardiographic parameters in advanced pulmonary arterial hypertension. Pulm Circ 2021;11:2045894021989966.
8. Sivakumar K. Atrial septal stenting – How I do it? Ann Pediatr Cardiol 2015;8:37-43.
9. Anderson JH, Cabalka AK, Frantz RP, Cajigas HR, Taggart NW. Transcatheter nonductal reverse potts shunt creation in pulmonary arterial hypertension. Circ Cardiovasc Interv 2022;15:e011315.
10. Mendel B, Christianto C, Angellia P, Holiyono I, Prakoso R, Siagian SN. Reversed potts shunt outcome in suprasystemic pulmonary arterial hypertension: A systematic review and meta-analysis. Curr Cardiol Rev 2022;18:e090522204486.
11. Lin CH, Huddleston C, Balzer DT. Transcatheter ventricular septal defect (VSD) creation for restrictive VSD in double-outlet right ventricle. Pediatr Cardiol 2013;34:743-7.
12. Meadows J, Pigula F, Lock J, Marshall A. Transcatheter creation and enlargement of ventricular septal defects for relief of ventricular hypertension. J Thorac Cardiovasc Surg 2007;133:912-8.
13. Khan JM, Rogers T, Greenbaum AB, Babaliaros VC, Yildirim DK, Bruce CG, *et al.* Transcatheter electrosurgery: JACC state-of-the-art review. J Am Coll Cardiol 2020;75:1455-70.
14. van Loon RL, Roofthooft MT, Hillege HL, ten Harkel AD, van Osch-Gevers M, Delhaas T, *et al.* Pediatric pulmonary hypertension in the Netherlands: Epidemiology and characterization during the period 1991 to 2005. Circulation 2011;124:1755-64.
15. Lowe BS, Therrien J, Ionescu-Ittu R, Pilote L, Martucci G, Marelli AJ. Diagnosis of pulmonary hypertension in the congenital heart disease adult population impact on outcomes. J Am Coll Cardiol 2011;58:538-46.
16. Humbert M, Sitbon O, Chaouat A, Bertocchi M, Habib G, Gressin V, *et al.* Pulmonary arterial hypertension in France: Results from a national registry. Am J Respir Crit Care Med 2006;173:1023-30.